

Determination of single-particle relaxation time from light scattering spectra in modulation-doped quantum wells

G. Fasol,* N. Mestres, M. Dobers, A. Fischer, and K. Ploog

Max-Planck-Institut für Festkörperforschung, Heisenbergstrasse 1, D-7000 Stuttgart 80, Federal Republic of Germany

(Received 2 March 1987)

We report Raman measurements of the k_{\parallel} dependence and temperature dependence of the imaginary part of the dielectric function of the electron gas in modulation-doped GaAs/Al_xGa_{1-x}As quantum wells. The Raman spectra are well explained by the Lindhard response function, using a phenomenological single-particle relaxation time τ_{sp} . We determine the temperature dependence of τ_{sp} .

I. THE 2D DIELECTRIC RESPONSE

The dielectric response function describes the response of a many-body system to external fields and is therefore of fundamental importance. Two-dimensional (2D) electron systems have attracted enormous interest recently and, accordingly, a very large number of theoretical papers¹⁻³ exist on the dielectric response of 2D and layered 2D electron systems, which mainly consider plasmon resonances.

Recent development of electronic Raman scattering techniques for the study of in-plane excitations in layered 2D electron systems^{4,5} have enabled us not only to study the plasmon resonances (the collective modes of excitation) but also the single-particle excitation spectra⁵ which are proportional to $\text{Im}[\chi_0(k_{\parallel}/\omega)]$. Since the single-particle excitation energies lie in a similar range as the thermal energies corresponding to usual low-temperature optical measurements, accurate determination and control of the temperature of the electronic system is crucial. This is done in the present work, and the methods are described in the experimental parts of this paper. This development opens the opportunity to study the single-particle excitations and their scattering and to compare them with theories for the dielectric function. We show in the present paper that a simple random-phase approximation (RPA) Lindhard-Mermin response function describes our data for the k_{\parallel} dependence and the temperature dependence of $\text{Im}(\chi_0)$. The present work takes specific advantage of the possibility of varying k_{\parallel} in a light scattering experiment of a 2D system. k_{\parallel} cannot be changed significantly in a 3D system except in a restricted range by changing the laser frequency. The single-particle excitations in bulk GaAs have been measured and interpreted using the Lindhard-Mermin response function in Ref. 6. At $T=0$ and without scattering, the single-particle excitation spectrum, and therefore $\text{Im}\epsilon$ has a triangular shape in a 3D electron gas, it has a sharply peaked shape in 2D, and it is a δ function at $\hbar k v_F$ in a 1D system.

Our measurements allow us to determine the single-particle (quantum) scattering time τ_{sp} . We attribute the increased width of the single-particle Raman spectra with respect to $\text{Im}\chi(\tau_{sp}=0)$ to the finite single-particle lifetime τ_{sp} . We determine a value for τ_{sp} by fitting the Lindhard-Mermin response function for the appropriate

electronic temperature T , determined by luminescence measurements, to our spectra. For the purpose of the present paper we identify τ_{sp} determined in this way with the single-particle relaxation time. As first pointed out by Mermin this approximation is phenomenological. For a more detailed understanding our data have to be interpreted using a detailed theory of the scattering processes. We should also point out at this stage that several different relaxation times may be defined for a particular system.

Harrang *et al.*⁷ have recently determined the quantum scattering time τ_{sdH} from Shubnikov-de Haas measurements. They show that comparison with the mobility scattering time τ_{μ} allows one to determine the dominating scattering process. This is because τ_{μ} is predominantly sensitive to large-angle scattering while τ_{sdH} is equally sensitive to all scattering angles. The ratio of τ_{sdH} to τ_{μ} therefore gives an indication of the angular properties of the scattering processes. τ_{sp} , which we determine here, is not equivalent to τ_{sdH} , since the latter depends on the assumption of a cutoff scattering angle.

The effects of scattering on the dielectric response (e.g., the plasma frequency and screening) of a 2D electron gas have been studied in a large number of papers. Of particular relevance to the present work is a recent calculation by Giuliani and Quinn.⁸ These authors have calculated microscopically the effect of scattering on the dielectric function (although δ function, i.e., isotropic, scattering) is assumed. They show that scattering drastically affects the plasma frequency in 2D at low frequencies. A microscopic justification of the Lindhard-Mermin function can also be deduced from the dielectric function of Ref. 8, supporting its use in the present work.

II. EXPERIMENTAL

For the present study we have investigated several different modulation-doped multiple quantum wells which show comparable results. In the present paper we show the spectra for the same sample as in Ref. 5, because this is the sample which we have best characterized and for the convenience of the reader. The structure of this sample consists of five modulation-doped quantum wells—each period consists of a 500-Å-wide GaAs quantum well surrounded by a 50-Å AlAs buffer layer on one side, a

100-Å $\text{Al}_{30}\text{Ga}_{70}\text{As}$ buffer layer on the other side, and a 250-Å Si-doped $\text{Al}_{30}\text{Ga}_{70}\text{As}$ layer between both buffer layers.

To interpret the single-particle excitation spectra it is crucial to know the 2D electron density per sheet of charge. Special attention has to be paid to the question of whether only the lowest subband is occupied. There are three effects which may render the interpretation difficult: Firstly, there may be two sheets of electrons in each of the 500-Å-wide wells—one close to each of the two interfaces; secondly, there may be an appreciable population of the first excited subband; and thirdly, the uppermost, or even several uppermost wells may be depleted due to pinning of the Fermi level due to defects on the surface of the sample structure.

For the present sample under saturating illumination we see at least thirty Shubnikov–de Haas (SdH) oscillations of ρ_{xx} as a function of $1/B$. The corresponding carrier density is $n = 6.85 \times 10^{11} \text{ cm}^{-2}$. Careful numerical analysis of the SdH data reveal a second period corresponding to $n = 0.9 \times 10^{11} \text{ cm}^{-2}$. The carrier density in these additional sheets of charge is small compared to the main contribution and will therefore be neglected in the present analysis. The SdH measurements show an additional period at *high magnetic* fields (of the order of 10 T), with a density about 10% lower, probably due to some depletion of the top layer or to effects of the upper conduction well levels. Since $k_F^{2D} \approx \sqrt{n}$, and since it only occurs at high fields, this effect has negligible consequences for the present results. For all samples which we studied in the course of this work we have studied the conduction intersubband separations both by Raman spectroscopy at the $E_0 + \Delta_0$ resonance and by luminescence excitation spectroscopy. For the present sample we interpret Raman and luminescence excitation measurements to yield $E_{01} \approx 24 \text{ meV}$. The value for the Fermi energy is expected to be $E_F^{2D} \approx 24 \text{ meV}$. Thus indeed only the lowest subband is expected to have significant occupation. The Raman signals around 10 meV appearing in parallel polarization (lines A, B, and C in Ref. 5) show different angular and laser wavelength dependence than the intersubband transitions measured in $E_0 + \Delta_0$ resonance. We are at present studying the origin of these lines using a number of samples. Self-consistent band-structure calculations will be necessary for a complete understanding of the subband structure, which we have not determined yet. We believe that our Shubnikov–de Haas measurements are convincing, that only the lowest subband is occupied significantly, and that the carrier density in all sheets of charge is very similar. We should point out that indeed in other comparable sample structures with higher carrier density we have observed a second period of oscillation, proving occupation of the first excited level. The period $\Delta(1/B)$ under saturated illumination yields a carrier density of $n = 6.85 \times 10^{11} \text{ cm}^{-2}$. The total carrier density determined from low-field Hall-effect measurement is $3.4 \times 10^{12} \text{ cm}^{-2}$. Assuming that five layers contribute, this yields a density of $n = 6.8 \times 10^{11} \text{ cm}^{-2}$ per layers, in excellent agreement with the SdH oscillation period. In addition, there is good agreement between the measured and the calculated plasmon dispersion for this

sample,⁵ and the position of the single-particle spectra is well described by $\hbar k_{\parallel} v_F$, where v_F depends only on the carrier density n in the lowest subband which is the only one which contributes significantly.

The fact that these four independent observations yield a consistent picture with the same carrier density shows that in the present sample a single sheet of charge per well contributes, that there are five sheets of charge in total, that the carrier density is $n = 6.8 \times 10^{11} \text{ cm}^{-2}$ per sheet, and that only the lowest subband has significant occupation. These observations are supported by the fact that the Fermi energy E_F is roughly the same as the intersubband separation E_{01} deduced from Raman experiments at $E_0 + \Delta_0$. For a final assignment self-consistent calculations will be done.

The Raman scattering equipment and our geometry has been described in Ref. 5. For an accurate study of single-particle excitations, which lie in the range 0–4 meV, corresponding to temperatures between 0 and 40 K, precise control and stability of the *electronic* temperature is crucial, particularly in view of the inevitable heating of the sample lattice and the electrons due to the laser illumination. We have monitored the stability of the cold-finger temperature throughout the measurement of each spectrum with a calibrated Ge resistor in thermal contact with the coldfinger close to the sample. We have determined the temperature of the electronic system by deter-

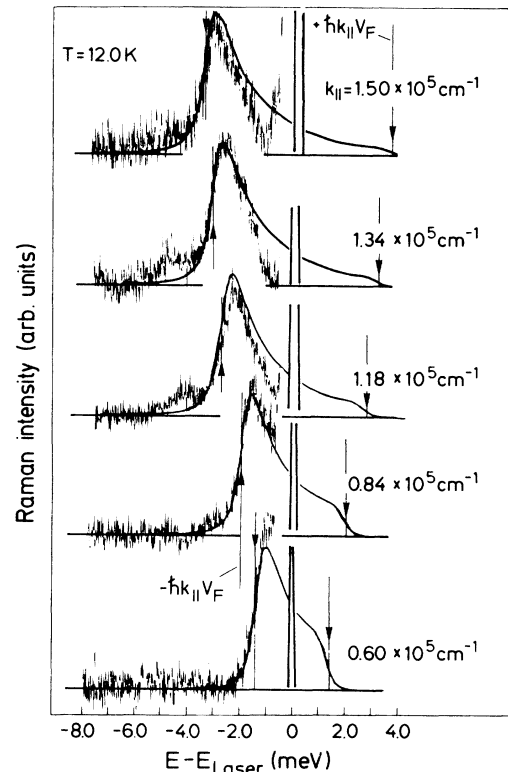


FIG. 1. Single-particle Raman scattering measured for the modulation-doped five-layer sample in crossed polarization. Spectra are shown for different in-plane wave-vector transfers k_{\parallel} . The solid curves are spectra calculated using the Lindhard-Mermin response function (see text).

mining the slope of the exponential high-energy tail of the quantum well luminescence. It is this temperature which we have used for the interpretation of our results. In addition, we checked the temperature determined from the luminescence measurements with the temperature determined from the ratio of the Stokes and anti-Stokes Raman spectra. In a typical measurement, where the laser power density falling onto the sample is 20 W cm^{-1} and the coldfinger temperature is 4.6 K we determine an electronic temperature of $7.5 \pm 0.5 \text{ K}$.

III. SPIN DENSITY FLUCTUATION SPECTRA

Figure 1 shows the single-particle Raman spectra measured for different values of k_{\parallel} with crossed polarization of incident and scattered light. Figure 2 shows the single-particle spectra measured with constant $k_{\parallel} = 1.33 \times 10^5 \text{ cm}^{-1}$ and for different temperatures. In this latter case we show both the Stokes and the anti-Stokes spectra. All spectra show on their Stokes side a peak which corresponds to the single-particle excitations, the high-energy shoulder lies at $\hbar k_{\parallel} v_F$. The value of $\hbar k_{\parallel} v_F$, determined from the carrier density is shown by the vertical arrow. Above this single-particle peak most spectra show a weak peak which occurs at the same energy as a plasmon resonance. We attribute this occurrence to the fact that the usual selection rules are not exactly valid in anisotropic quantum well samples. All spectra

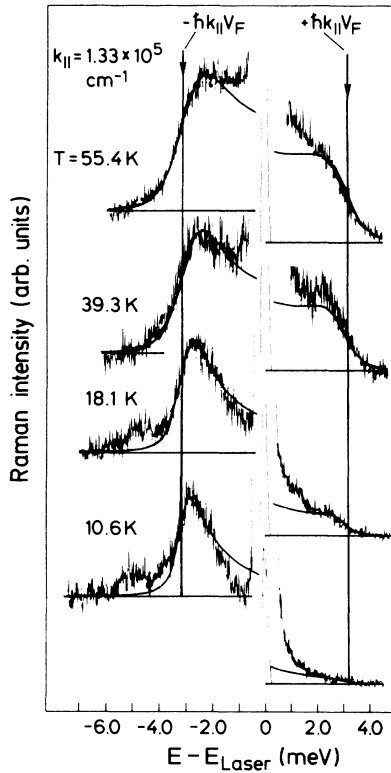


FIG. 2. Temperature dependence of single-particle Raman spectra. The different background of Stokes and anti-Stokes spectra is attributed to a hot luminescence background. The solid curves are spectra calculated using the Lindhard-Mermin response function (see text).

show a background which is larger for the Stokes than the anti-Stokes side which we attribute to hot luminescence. The spectrum for $T = 39.3 \text{ K}$ is measured at a higher dye laser energy than the other spectra, and shows a much smaller luminescence background.

The spectra taken here are all measured in crossed polarization. In this case the light scattering is due to spin-density fluctuations. As calculated by Hamilton and McWhorter⁹ for GaAs, the spectra in this case are proportional to $\text{Im}[\chi_0(k_{\parallel}, \omega)]$.

To interpret our results we have calculated $\text{Im}[\chi(k_{\parallel}, \omega)]$ using

$$\chi(k_{\parallel}, \omega) = \frac{(1 + i/\omega\tau_{\text{sp}})[\chi_0(k_{\parallel}, \omega + i/\tau_{\text{sp}})]}{1 + (i/\omega\tau_{\text{sp}})[\chi_0(k_{\parallel}, \omega + i/\tau_{\text{sp}})/\chi_0(k_{\parallel}, 0)]} \quad (1)$$

from Ref. 10 and

$$\chi_0(k_{\parallel}, \omega) = \frac{e^2}{k_{\parallel}\Omega} \int d^2q \frac{f_0(E_q) - f_0(E_{q+k_{\parallel}})}{E_{q+k_{\parallel}} - E_q - \hbar\omega} \quad (2)$$

from Ref. 11. f_0 is the Fermi-Dirac function for the appropriate electronic temperature. While Stern² has evaluated the integral in Eq. (2) analytically at $T=0$, we have calculated the integral numerically for the appropriate electron temperature. The calculation by Mermin¹⁰ of Eq. (1) applies to the two-dimensional case, since the dimensionality only appears in executing the integrals.

In each case, we have determined the single-particle relaxation time τ_{sp} , for which the best fit is achieved. The solid lines in Figs. 1 and 2 are fits of

$$\frac{d^2\sigma}{d\Omega d\omega} \approx (1 - e^{-\hbar\omega/k_B T})^{-1} \text{Im}\chi(k_{\parallel}, \omega) \quad (3)$$

(Eq. 2.92 from Ref. 12), where $\chi(k_{\parallel}, \omega)$ is calculated numerically from Eqs. (1) and (2) for those values of τ_{sp} which yield the best fit. The calculated spectra are shown as the solid curves in Figs. 1 and 2 and are shifted by the background of each spectrum. The agreement of the calculated spectra with the measured spectra is remarkably good, if one considers the simplicity of this theory.

In Fig. 3 we have plotted the temperature dependence of the single-particle relaxation rate $1/\tau_{\text{sp}}$ and we compare it with the mobility relaxation rate $1/\tau_{\mu}$ determined from the Hall mobility. Extrapolating to $T=0$ we find $\tau_{\text{sp}}(T=0) = 1.8 \pm 0.3 \text{ ps}$ and $\tau_{\mu}(T=0) = 7.1 \pm 0.1 \text{ ps}$, and therefore $\tau_{\mu}/\tau_{\text{sp}} = 4.0 \pm 0.8$. The fact that the single-particle quantum relaxation rate is considerably higher than the mobility scattering rate shows that small-angle scattering contributes to a large extent to the total scattering.

Our results may be compared with the theoretical work by Das Sarma and Stern¹³ and the work by Harrang *et al.*,⁷ where the quantum scattering time was determined from SdH measurements. In this work it was shown that the high value of $\tau_{\mu}/\tau_{\text{SdH}}$ is attributed to scattering from impurities remote from the electron channel. For a detailed comparison of the various scattering times microscopic theories (e.g., Refs. 8 or 13) of the scattering are necessary.

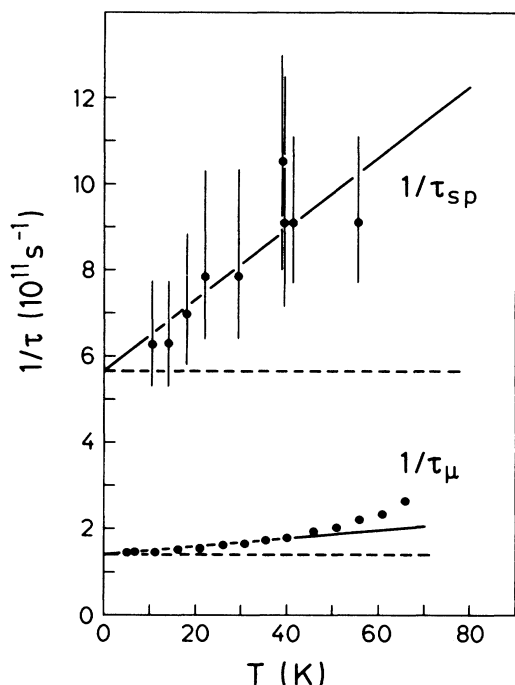


FIG. 3. Inverse mobility relaxation time $1/\tau_\mu$ and inverse single-particle relaxation time $1/\tau_{sp}$ as a function of temperature. τ_{sp} is determined by the best fit of Eq. (3) to the spectra. The dashed lines show the contribution to the total scattering rates attributed to impurity scattering, while the solid lines are least-squares fits.

Up to 50 K the mobility rate $1/\tau_\mu$ rises linearly with a slope of $\alpha_\mu = 3.9 \times 10^{-8}$ V s/cm² K. This linear slope is attributed to acoustic phonon scattering and agrees well with recent work.^{14,15} The positive slope confirms that impurity scattering is low in our samples. The single-particle rate $1/\tau_{sp}$ rises much faster with temperature which is expected since acoustic scattering is mainly forward. Its slope is $\alpha_{sp} = 3.1 \times 10^{-7}$ V s/cm² K. Therefore $\alpha_{sp}/\alpha_\mu = 8.2$. This drastic difference in temperature dependence may in addition be affected by the temperature dependence of the screening.¹⁶

We should make one more comment. The single-particle excitations studied optically are at considerably higher energy from the Fermi sphere than the excitations relevant for transport measurements.¹⁷ Since impurity scattering, which is the only scattering contribution at $T=0$, is elastic scattering, and since the density of states as a function of energy in two dimensions is constant, the phase space of final states for τ_{sp} events and for τ_μ events is the same. At high enough energies above E_F the lifetime of the quasiparticles due to electron-electron scattering may start to play a role.

IV. CONCLUSIONS

In conclusion, we have shown that accurate measurements of the Raman spectra due to spin-density fluctuations allow us to study the single-particle excitation spectra, their $k_{||}$, and their temperature dependence. We show that a simple RPA theory incorporating a phenomenological single-particle relaxation time τ_{sp} explains our spectra remarkably well although there are some deviations, which we have attributed to luminescence background. The deviations may also turn out to be a manifestation of exchange and correlation effects. We determine the ratio of the impurity scattering components of the mobility relaxation time τ_μ , determined from Hall measurements and τ_{sp} and find that it greatly exceeds 1. For our particular sample we find $\tau_\mu/\tau_{sp} = 4.0 \pm 0.8$ for the impurity related rates. Such a high value of τ_μ/τ_{sp} is characteristic of remote impurity scattering, where small-angle scattering events are particularly important. Our results confirm recent work^{7,13} in this respect. We find a much stronger temperature dependence of the single-particle scattering rate than the rate relevant for the mobility.

ACKNOWLEDGMENTS

We express our deep gratitude to M. Cardona for numerous discussions and his help and support and a critical reading of the manuscript and to D. Heitmann, R. Haug, K. von Klitzing, and G. Lonzarich for numerous helpful discussions. The technical assistance of M. Siemers, H. Hirt, and P. Wurster is gratefully acknowledged.

*Present address: Cavendish Laboratory, Madingley Road, Cambridge CB3 0HE, United Kingdom.

¹R. H. Ritchie, Phys. Rev. **106**, 875 (1957); R. A. Ferrel, *ibid.* **111**, 1214 (1958).

²F. Stern, Phys. Rev. Lett. **18**, 546 (1967).

³See, for example, S. Das Sarma and J. J. Quinn, Phys. Rev. B **25**, 7603 (1982); J. K. Jain and P. B. Allen, *ibid.* **32**, 997 (1985), and references therein.

⁴D. Olego, A. Pinczuk, A. C. Gossard, and W. Wiegmann, Phys. Rev. B **26**, 7867 (1982); R. Sooryakumar, A. Pinczuk, A. Gossard, and W. Wiegmann, *ibid.* **31**, 2578 (1985); A. Pinczuk, M. G. Lamont, and A. C. Gossard, Phys. Rev. Lett. **26**, 2092 (1986).

⁵G. Fasol, N. Mestres, H. P. Hughes, A. Fischer, and K. Ploog,

Phys. Rev. Lett. **56**, 2517 (1986).

⁶A. Pinczuk, G. Abstreiter, R. Trommer, and M. Cardona, Solid State Commun. **30**, 429 (1979).

⁷J. P. Harrang, R. J. Higgins, R. K. Goodall, P. R. Jay, M. Laviron, and P. Delescluse, Phys. Rev. B **32**, 8126 (1985).

⁸G. F. Giuliani and J. J. Quinn, Phys. Rev. **29**, 2321 (1984).

⁹D. C. Hamilton and A. L. McWhorter, in *Light Scattering Spectra of Solids*, edited by G. B. Wright (Springer-Verlag, Berlin, 1969), p. 309.

¹⁰N. D. Mermin, Phys. Rev. **1**, 2362 (1970).

¹¹J. Lindhard, Dan. Mat. Fys. Medd. **28**, 1 (1954).

¹²G. Abstreiter, M. Cardona, and A. Pinczuk, in *Light Scattering in Solids IV*, edited by M. Cardona and G. Güntherodt (Springer-Verlag, Heidelberg, 1984), p. 5.

¹³S. Das Sarma and F. Stern, Phys. Rev. B **32**, 8442 (1985).

¹⁴E. E. Mendez, P. J. Price, and M. Heiblum, Appl. Phys. Lett. **45**, 294 (1984).

¹⁵B. I. F. Lin, D. C. Tsui, and G. Weimann, Solid State Com-

mun. **56**, 287 (1985).

¹⁶C. Guillemot, Phys. Rev. B **31**, 1428 (1985).

¹⁷We are very grateful to H. Störmer for commenting on this point.